

Relative Fuzzy Connectedness on Directed Graphs and its Application in a Hybrid Method for Interactive Image Segmentation

Hans H.C. Bejar, Paulo A.V. Miranda
Department of Computer Science,
University of São Paulo (USP),
05508-090, São Paulo, SP, Brazil.

Email: hans@ime.usp.br pmiranda@vision.ime.usp.br

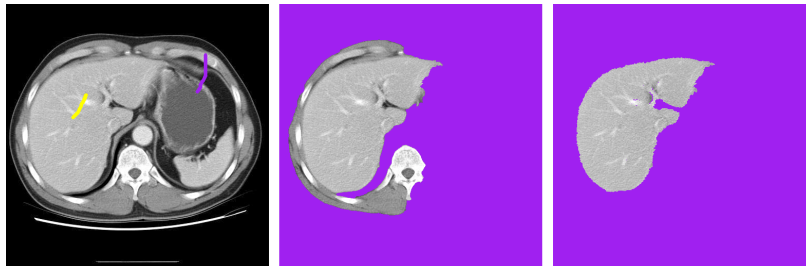


Figure 1. An example result highlighting the effectiveness of our method: A CT slice image of the liver with user-selected markers (left). The segmentation result by Oriented Image Foresting Transform invades some background regions (middle). A better result is obtained by the proposed Oriented Relative Fuzzy Connectedness method (right).

Abstract—Anatomical structures and tissues are often hard to be segmented in medical images due to their poorly defined boundaries, i.e., low contrast in relation to other nearby false boundaries. The specification of the boundary polarity can help to alleviate part of this problem. In this work, we discuss how to incorporate this property in the Relative Fuzzy Connectedness (RFC) framework. We present a new algorithm, named Oriented Relative Fuzzy Connectedness (ORFC), in terms of an oriented energy function subject to the seed constraints, and its application in powerful hybrid segmentation methods. The hybrid method proposed ORFC&Graph Cut preserves the robustness of ORFC respect to the seed choice, avoiding the shrinking problem of Graph Cut (GC), and keeps the strong control of the GC in the contour delineation of irregular image boundaries. The proposed methods are evaluated using medical images of MRI and CT images of the human brain and thoracic studies.

Keywords—Relative fuzzy connectedness, image foresting transform, graph-cut segmentation, graph search algorithms.

I. INTRODUCTION

In this work, we explore graphs by modeling neighborhood relationships of picture elements from digital images for the purposes of image segmentation, such as to extract an object from a background, by assigning different labels to its picture elements.

One important class of graph-based image segmentation methods comprises interactive seed-based methods, including different frameworks, such as fuzzy connectedness [1], graph

cuts [4], and image foresting transform [5]. The study of the relations among different frameworks, including theoretical and empirical comparisons, has a vast literature [6], [7], [8], [9], which allowed many algorithms to be described in a unified manner according to a common framework, which we refer to as, Generalized GC (GGC) [10]. Within this framework, there are two important classes of energy formulations, the ε_1 - and ε_∞ -minimization problems (and so, the associated algorithms), as discussed in [10]. The most efficient seed-based approaches of the GGC framework are the ones that fall within the ε_∞ -minimization problem, which have linear-time implementations $O(N)$ with respect to the image size N [7], while the run time for the ε_1 -minimization problem is $O(N^{2.5})$ for sparse graphs [11]. Some methods from the ε_∞ -minimization family were extended to support the boundary-polarity constraint, by exploring directed weighted graphs, leading to the method named *Oriented Image Foresting Transform* (OIFT) [2], [12]. While the introduction of combinatorial graphs with directed edges on other frameworks increases considerably the complexity of the problem [13], OIFT still runs in linear time. The boundary orientation information is crucial for effective automatic segmentation, as demonstrated by boundary-based approaches [14]. In this work, we discuss how to incorporate this orientation information, by exploring digraphs, in another member of the ε_∞ -minimization family, a region-based approach called Relative Fuzzy Connectedness (RFC) [15]. RFC is an important method, which presents some

¹This work is related to a M.Sc. dissertation.

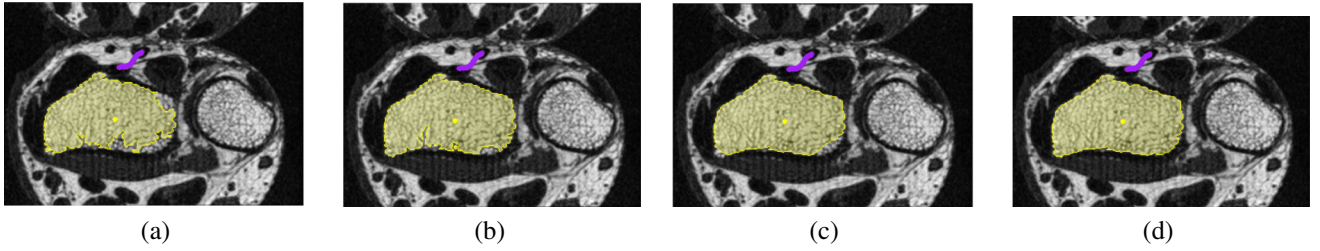


Figure 2. An example result of ORFC+GC. The segmentation of the wrist by: (a) IRFC [1], (b) OIFT [2], (c) RFC+GC [3], and (d) ORFC+GC.

nice theoretical properties, such as the robustness with respect to the seed choice [15].

We propose a new method, named *Oriented Relative Fuzzy Connectedness* (ORFC), which allow the customization of the segmentation by RFC to match global features of a target object, by considering the orientation of the object’s intensity transitions, i.e., bright to dark or the opposite (boundary polarity). We also extend the hybrid approach [3] to directed weighted graphs, incorporating the boundary polarity by combining the strengths of oriented relative fuzzy connectedness and graph cut. The novel hybrid approach is more robust than the original graph cut with respect to the seed choice (thus, avoiding “shrinking problem” of GC), it also outperforms the previous hybrid method [3] and OIFT, with running times close to linear.

Section II explains the basic concepts on image graphs, and introduces the terminology and notation to be used throughout the text. The proposed extension of RFC, named Oriented Relative Fuzzy Connectedness, is presented in Section III and its applications in hybrid image segmentation (ORFC and graph cut) are shown in Section IV. Sections V and VI discuss the experimental results and conclusions.

II. BACKGROUND

A multi-dimensional and multi-spectral image \hat{I} is a pair (\mathcal{I}, \vec{I}) where $\mathcal{I} \subset \mathbb{Z}^n$ is the image domain and $\vec{I}(a)$ assigns a set of m scalars $I_i(a)$, $i = 1, 2, \dots, m$, to each pixel $a \in \mathcal{I}$. The subindex i is removed when $m = 1$.

An image can be interpreted as a weighted digraph $G = (\mathcal{V}, E, w)$ whose nodes \mathcal{V} are the image pixels in its image domain $\mathcal{I} \subset \mathbb{Z}^n$, and whose arcs are the ordered pixel pairs $\langle a, b \rangle \in E$. For example, one can take E to consist of all pairs of pixels $\langle a, b \rangle$ in the Cartesian product $\mathcal{I} \times \mathcal{I}$ such that $d(a, b) \leq \rho$ and $a \neq b$, where $d(a, b)$ denotes the Euclidean distance and ρ is a specified constant (e.g., 4-neighborhood, when $\rho = 1$, and 8-neighborhood, when $\rho = \sqrt{2}$, in case of 2D images). The digraph G is symmetric if for any of its arcs $\langle a, b \rangle$, the pair $\langle b, a \rangle$ is also an arc of G . Each arc $\langle a, b \rangle \in E$ has a fixed weight $w(a, b) \geq 0$, between neighboring pixels, which is ideally designed to have lower values in the boundary transitions of the object of interest (e.g., $w(a, b) = K - |I(a) - I(b)|$, where K is the greatest difference in image brightness for a single channel image with values given by $I(a)$). A symmetric digraph is undirected weighted

if $w(a, b) = w(b, a)$ for all $\langle a, b \rangle \in E$, otherwise we have a directed weighted digraph.

The transpose $G^T = (\mathcal{V}, E^T, w^T)$ of a weighted digraph $G = (\mathcal{V}, E, w)$, for any of its arcs $\langle a, b \rangle \in E^T$, the pair $\langle b, a \rangle$ is an arc of G , and $w^T(a, b) = w(b, a)$. A weighted digraph G is symmetric and undirected weighted if G is the same as its transpose.

For a given image graph $G = (\mathcal{V}, E, w)$, a path $\pi_a = \langle t_1, t_2, \dots, t_n = a \rangle$ is a sequence of adjacent pixels with terminus at a pixel a . A path is *trivial* when $\pi_a = \langle a \rangle$. A path $\pi_b = \pi_a \cdot \langle a, b \rangle$ indicates the extension of a path π_a by an arc $\langle a, b \rangle$. When we want to explicitly indicate the origin of a path, the notation $\pi_{a \rightsquigarrow b} = \langle t_1 = a, t_2, \dots, t_n = b \rangle$ may also be used, where a stands for the origin and b for the destination node. More generally, we can use $\pi_{S \rightsquigarrow b} = \langle t_1, t_2, \dots, t_n = b \rangle$ to indicate a path with origin restricted to a set S (i.e., $t_1 \in S$). A digraph is said to be *strongly connected* if there is a path from every vertex to every other vertex. A *connectivity function* computes a value $f(\pi_a)$ for any path π_a , usually based on arc weights. A path π_a is *optimum* if $f(\pi_a) \geq f(\tau_a)$ for any other path τ_a in G .

For every weighted digraph $G = (\mathcal{V}, E, w)$, consider the space \mathcal{X} of all functions $x: \mathcal{V} \rightarrow [0, 1]$, referred to as *fuzzy subsets* of \mathcal{V} , with the value $x(a)$ indicating a degree of membership with which a belongs to the set. The family \mathcal{X} of all functions $x \in \mathcal{X}$ with the only allowed values of 0 and 1 (i.e., $x: \mathcal{V} \rightarrow \{0, 1\}$) will be referred to as the family of all *hard subsets* of \mathcal{V} . Each $x \in \mathcal{X}$ is identified with the true subset $P = \{c \in \mathcal{V}: x(c) = 1\}$ of \mathcal{V} . Notice that, in such a case, x is the *characteristic function* χ_P of $P \subset \mathcal{V}$. We usually restrict the collection \mathcal{X} of all allowable objects by indicating two disjoint sets, referred to as *seeds*: $\mathcal{S}_o \subset \mathcal{V}$ indicating the object and $\mathcal{S}_b \subset \mathcal{V}$ indicating the background.

This restricts the collection of allowable outputs of the algorithm to the family $\mathcal{X}(\mathcal{S}_o, \mathcal{S}_b)$ of all $x \in \mathcal{X}$ with $x(a) = 1$ for all $a \in \mathcal{S}_o$, and $x(b) = 0$ for all $b \in \mathcal{S}_b$. Note that $\mathcal{X}(\mathcal{S}_o, \mathcal{S}_b) = \{\chi_P: \mathcal{S}_o \subset P \subset \mathcal{V} \setminus \mathcal{S}_b\}$.

We consider the following connectivity function:

$$f_{\min}^{\mathcal{S}}(\langle a \rangle) = \begin{cases} w_{max} + 1 & \text{if } a \in \mathcal{S} \\ -\infty & \text{otherwise} \end{cases}$$

$$f_{\min}^{\mathcal{S}}(\pi_a \cdot \langle a, b \rangle) = \min\{f_{\min}^{\mathcal{S}}(\pi_a), w(a, b)\}$$

where $w_{max} = \max_{\langle a, b \rangle \in E} w(a, b)$.

III. ORIENTED RELATIVE FUZZY CONNECTEDNESS (ORFC)

Differently from RFC [16], [7], [9], the definitions of ORFC based on paths and based on cuts in the digraph lead to different results. The different obtained algorithms will be denoted as $A_{ORFC}^{in, \rightsquigarrow}$, and $A_{ORFC}^{out, \rightsquigarrow}$ for the path-based definition; and $A_{ORFC}^{in, \bowtie}$, and $A_{ORFC}^{out, \bowtie}$ for the cut-based definition.

A. ORFC definition by reverse connectivity functions

Based on the previous works [2], [12], we consider the following new connectivity function in digraphs:

$$f_{\min}^{\mathcal{W}S}(\langle a \rangle) = \begin{cases} w_{max} + 1 & \text{if } a \in \mathcal{S} \\ -\infty & \text{otherwise} \end{cases}$$

$$f_{\min}^{\mathcal{W}S}(\pi_a \cdot \langle a, b \rangle) = \min\{f_{\min}^{\mathcal{W}S}(\pi_a), w(b, a)\}$$

where $\langle b, a \rangle$ is an anti-parallel arc.

Note that $f_{\min}^{\mathcal{W}S}$ is a smooth function, and therefore $V_o^{\mathcal{W}}$ and $V_b^{\mathcal{W}}$ are optimum connectivity maps. These two connectivity maps are generated by executing the IFT with anti-parallel connectivity functions:

$$V_o(a) = \max_{\pi_a \in \Pi(G, a)} \{f_{\min}^{\mathcal{S}_o}(\pi_a)\}; V_o^{\mathcal{W}}(a) = \max_{\pi_a \in \Pi(G, a)} \{f_{\min}^{\mathcal{W}S_o}(\pi_a)\}$$

$$V_b(a) = \max_{\pi_a \in \Pi(G, a)} \{f_{\min}^{\mathcal{S}_b}(\pi_a)\}; V_b^{\mathcal{W}}(a) = \max_{\pi_a \in \Pi(G, a)} \{f_{\min}^{\mathcal{W}S_b}(\pi_a)\}$$

Following the same key idea from [2] (i.e., to consider reversed connectivity functions for one of the seed sets), we have the following natural definition for ORFC: The segmentation $A_{ORFC}^{out, \rightsquigarrow}(\mathcal{S}_o, \mathcal{S}_b)$ favoring transitions from bright to dark pixels is obtained by comparing the connectivity maps $V_o(a)$ and $V_b^{\mathcal{W}}(a)$, such that each pixel $a \in \mathcal{V}$ is labeled as belonging to the object only if $V_o(a) > V_b^{\mathcal{W}}(a)$.

$$A_{ORFC}^{out, \rightsquigarrow}(\mathcal{S}_o, \mathcal{S}_b) = \chi_O : O = \{a \in \mathcal{V} : V_o(a) > V_b^{\mathcal{W}}(a)\} \quad (1)$$

The segmentation $A_{ORFC}^{in, \rightsquigarrow}(\mathcal{S}_o, \mathcal{S}_b)$ favoring transitions from dark to bright pixels is obtained by comparing the connectivity maps $V_o^{\mathcal{W}}(a)$ and $V_b(a)$, such that each pixel $a \in \mathcal{V}$ is labeled as belonging to the object only if $V_o^{\mathcal{W}}(a) > V_b(a)$.

$$A_{ORFC}^{in, \rightsquigarrow}(\mathcal{S}_o, \mathcal{S}_b) = \chi_O : O = \{a \in \mathcal{V} : V_o^{\mathcal{W}}(a) > V_b(a)\} \quad (2)$$

Note that although this ORFC version is based on optimum connectivity maps, its practical results have undesirable characteristics, such as the presence of disconnected regions and high false-positive rates, leading to unsatisfactory results.

B. ORFC as a directed cut in the digraph

Given that the previous ORFC definition (Section III-A) presents undesirable results, in this section we present an alternative definition supported by a graph cut optimality criterion, which is motivated by the definitions from RFC [7].

Differently from RFC, in the case of directed graphs, we have two possible sets of cuts (Figure 3):

$$C_{out}(x) = \{\langle a, b \rangle \in E : x(a) = 1 \wedge x(b) = 0\} \quad (3)$$

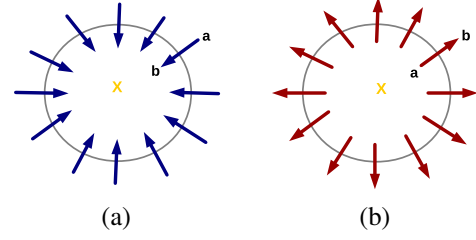


Figure 3. The two possible sets of cuts. The inner and outer cuts for a candidate object showing the input and output arcs.

$$C_{in}(x) = \{\langle a, b \rangle \in E : x(a) = 0 \wedge x(b) = 1\} \quad (4)$$

So we have two possible formulations for the energy functional of the ε_∞ -minimizing problem.

$$\varepsilon_\infty^{out}(x) = \max_{\langle a, b \rangle \in C_{out}} w(a, b) \quad (5)$$

$$\varepsilon_\infty^{in}(x) = \max_{\langle a, b \rangle \in C_{in}} w(a, b) \quad (6)$$

Let $\varepsilon_{\infty\downarrow}^{out}$ be the minimum value of the energy $\varepsilon_\infty^{out}(x)$, that is:

$$\varepsilon_{\infty\downarrow}^{out} = \min\{\varepsilon_\infty^{out}(x) : x \in \mathcal{X}(\mathcal{S}_o, \mathcal{S}_b)\} \quad (7)$$

Similarly, for $\varepsilon_\infty^{in}(x)$, we have:

$$\varepsilon_{\infty\downarrow}^{in} = \min\{\varepsilon_\infty^{in}(x) : x \in \mathcal{X}(\mathcal{S}_o, \mathcal{S}_b)\} \quad (8)$$

Therefore, we have the following sets of solutions:

$$\mathcal{X}_\infty^{out}(\mathcal{S}_o, \mathcal{S}_b) = \{x \in \mathcal{X}(\mathcal{S}_o, \mathcal{S}_b) : \varepsilon_\infty^{out}(x) = \varepsilon_{\infty\downarrow}^{out}\} \quad (9)$$

$$\mathcal{X}_\infty^{in}(\mathcal{S}_o, \mathcal{S}_b) = \{x \in \mathcal{X}(\mathcal{S}_o, \mathcal{S}_b) : \varepsilon_\infty^{in}(x) = \varepsilon_{\infty\downarrow}^{in}\} \quad (10)$$

The ORFC algorithms on digraphs have the following definitions based on cut in graph:

For the outer cut “out” with one internal seed s_1 ,

$$A_{ORFC}^{out, \bowtie}(\{s_1\}, \mathcal{S}_b) = \chi_O \in \mathcal{X}_\infty^{out}(\{s_1\}, \mathcal{S}_b) : |O| = \min\{|P| : \chi_P \in \mathcal{X}_\infty^{out}(\{s_1\}, \mathcal{S}_b)\} \quad (11)$$

and in the case of multiple internal seeds,

$$A_{ORFC}^{out, \bowtie}(\mathcal{S}_o, \mathcal{S}_b) = \chi_O : O = \left[\bigcup_{s_i \in \mathcal{S}_o} P : \chi_P = A_{ORFC}^{out, \bowtie}(\{s_i\}, \mathcal{S}_b) \right] \quad (12)$$

For the inner cut “in” with one internal seed s_1 ,

$$A_{ORFC}^{in, \bowtie}(\{s_1\}, \mathcal{S}_b) = \chi_O \in \mathcal{X}_\infty^{in}(\{s_1\}, \mathcal{S}_b) : |O| = \min\{|P| : \chi_P \in \mathcal{X}_\infty^{in}(\{s_1\}, \mathcal{S}_b)\} \quad (13)$$

and in the case of multiple internal seeds,

$$A_{ORFC}^{in, \bowtie}(\mathcal{S}_o, \mathcal{S}_b) = \chi_O : O = \left[\bigcup_{s_i \in \mathcal{S}_o} P : \chi_P = A_{ORFC}^{in, \bowtie}(\{s_i\}, \mathcal{S}_b) \right] \quad (14)$$

C. ORFC algorithm based on graph cut

In order to show the proposed algorithms, we need the following definition:

Definition 1 (Directed Connected Component). For a given vertex x of a digraph G , the directed connected component of basepoint x is the set, denoted by $DCC_G(x)$, of all the successors of x in G (i.e., all the nodes that are reachable from vertex x by some path).

Algorithm 1:

Algorithm to compute $A_{ORFC}^{in, \infty}(\{s_i\}, S_b)$:

- 1) Compute the value of the map $V_b(s_i)$ for the function $f_{min}^{S_b}$.
- 2) Remove from the graph G all edges with weight $\leq \varepsilon_{\infty \downarrow}^{in} = V_b(s_i)$, obtaining a new graph G_{\leq} .
- 3) Assign to the object the pixels that belong to the directed connected component of basepoint s_i in the transpose graph of G_{\leq} (i.e., $A_{ORFC}^{in, \infty}(\{s_i\}, S_b) = \chi_O: O = DCC_{G_{\leq}^T}(s_i)$).

Figure 4 illustrates the steps of Algorithm 1.

Algorithm 2:

Algorithm to compute $A_{ORFC}^{out, \infty}(\{s_i\}, S_b)$:

- 1) Compute the value of the map $V_b^{\#}(s_i)$ for the function $f_{min}^{\# S_b}$.
- 2) Remove from the graph G all edges with weight $\leq \varepsilon_{\infty \downarrow}^{out} = V_b^{\#}(s_i)$, obtaining a new graph G_{\leq} .
- 3) Assign to the object the pixels that belong to the directed connected component of basepoint s_i in the graph G_{\leq} (i.e., $A_{ORFC}^{out, \infty}(\{s_i\}, S_b) = \chi_O: O = DCC_{G_{\leq}}(s_i)$).

IV. HYBRID SEGMENTATION: ORFC & GRAPH CUT

In this section, we follow the same key ideas from [3], which proposes a hybrid approach combining the strengths of relative fuzzy connectedness and min-cut/max-flow algorithm.

The graph cut (GC) natively supports the soft constraint of boundary polarity, and will be denoted as oriented graph cut (OGC). It ($A_{OGC}^{out}(\mathcal{S}_o, \mathcal{S}_b)$) solves the ε_1 -minimization problem by considering the arcs that limit the flow from the source to the sink, and consequently minimizes the sum of the edges pointing from object to background pixels (i.e., the outer cut) [4]. The minimization of the sum of the arcs of the inner cut ($A_{OGC}^{in}(\mathcal{S}_o, \mathcal{S}_b)$) can be obtained by inverting the source and sink nodes, or by reversing all arcs by computing GC over the graph's transpose G^T .

Basically, by considering in [3] a directed weighted graph, with ORFC in place of RFC, we have the ORFC + GC hybrid approach (Figure 2) as follows:

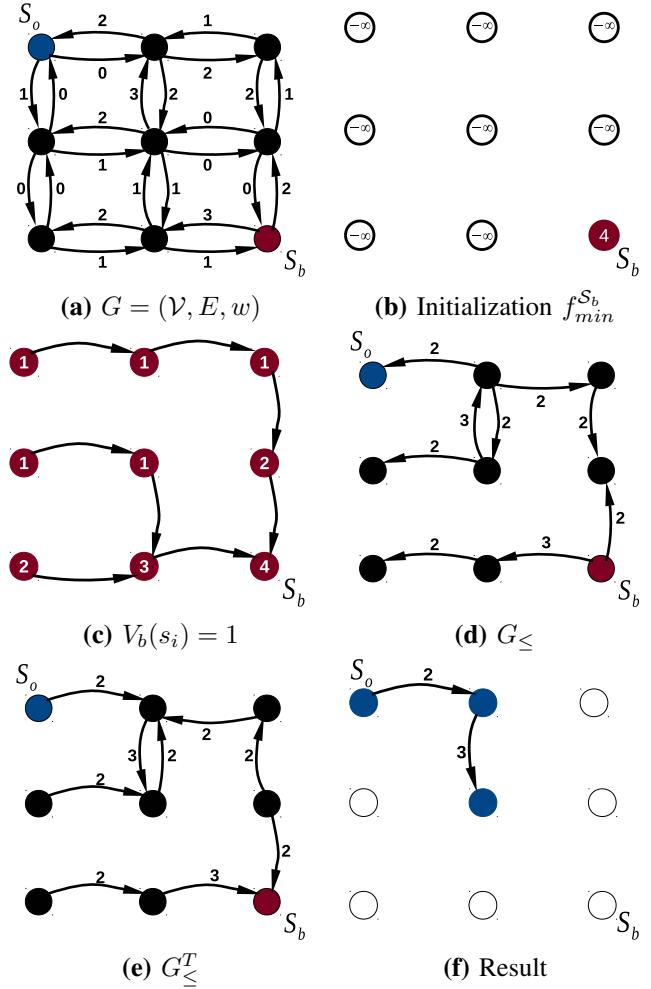


Figure 4. Algorithm $A_{ORFC}^{in, \infty}(\mathcal{S}_o = \{s_i\}, \mathcal{S}_b)$. (a) Image as a digraph. (b) Initialization of IFT with background seed \mathcal{S}_b for computing the connectivity value $V_b(s_i)$ using the connectivity function $f_{min}^{S_b}$. (c) Result of step 1: The value $V_b(s_i) = 1$ is computed by IFT. (d) Step 2: the graph G_{\leq} . (e,f) Step 3: The transpose graph of G_{\leq} and finally, the object's pixels from the DCC.

Algorithm 3:

Algorithm to compute $A_{ORFC+GC}^{in, \infty}(\mathcal{S}_o, \mathcal{S}_b)$:

- 1) Compute P : $\chi_P = A_{ORFC}^{in, \infty}(\mathcal{S}_o, \mathcal{S}_b)$.
- 2) Compute Q : $\chi_Q = A_{ORFC}^{out, \infty}(\mathcal{S}_b, \mathcal{S}_o)$.
- 3) Compute and return $A_{OGC}^{in}(P, Q)$.

Algorithm 4:

Algorithm to compute $A_{ORFC+GC}^{out, \infty}(\mathcal{S}_o, \mathcal{S}_b)$:

- 1) Compute P : $\chi_P = A_{ORFC}^{out, \infty}(\mathcal{S}_o, \mathcal{S}_b)$.
- 2) Compute Q : $\chi_Q = A_{ORFC}^{in, \infty}(\mathcal{S}_b, \mathcal{S}_o)$.
- 3) Compute and return $A_{OGC}^{out}(P, Q)$.

Figure 5 illustrates the steps of Algorithm 4.

V. EXPERIMENTAL RESULTS

In the first experiment, we used 40 slice images from real MR images of the foot and 40 slice images from CT thoracic (Figure 6). We performed the segmentation of the liver and

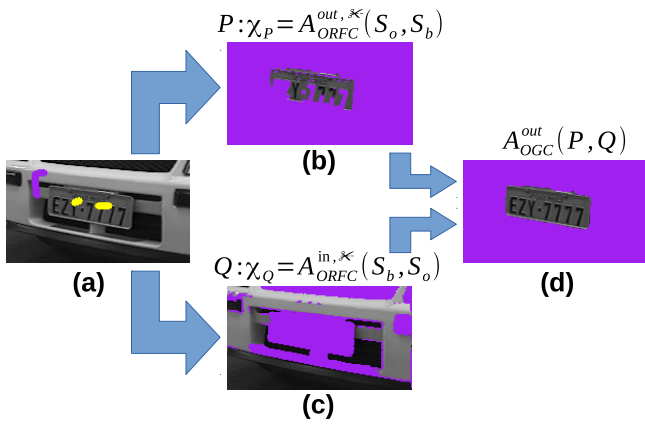


Figure 5. Algorithm $A_{ORFC+GC}^{out, \kappa}(S_o, S_b)$. (a) Input image with seeds S_o e S_b (b) $P: X_P = A_{ORFC}^{out, \kappa}(S_o, S_b)$. (c) $Q: X_Q = A_{ORFC}^{in, \kappa}(S_b, S_o)$. (d) $A_{OGC}^{out}(P, Q)$.

bones calcaneus and talus for all the methods (*IRFC* [1], *RFC* [15], *OIFT* [12], *RFC+GC* [3], *OGC* [4] - the graph cut with boundary polarity, *ORFC*, and the proposed hybrid method *ORFC+GC*), for different seed sets automatically obtained by eroding and dilating the ground truth at different radius values. By varying the radius value, we can repeat the segmentation for different seed sets and trace accuracy curves using the Dice coefficient of similarity, and error curves of false positive (normalized by the object size). However, in order to generate a more challenging situation, we considered a larger radius of dilation for the external seeds (twice the value of the inner radius), resulting in an asymmetrical arrangement of seeds.

We also repeated the experiments using two three-dimensional datasets (Figure 7). In the former case, a MRI-T1 dataset of 20 human brain was used to segment the cerebellum. The images were acquired with a 2T Elscint scanner and at a voxel size of $0.98 \times 0.98 \times 1.00 \text{ mm}^3$, for the second dataset, we considered a skull stripping task (Figure 8) (i.e., to eliminate background, bones, eyes, skin, and blood vessels) using ten 3 Tesla MRI-T1 images. The *RFC* and *ORFC* methods performed poorly on these datasets due to the lack of a clear contrast between the structures. We considered $\alpha = 0.5$ (orientation factor that was used to calculate the digraph from the undirected graph) in all experiments involving *OIFT*, *OGC*, *ORFC*, and *ORFC+GC*; and $\alpha = 0.0$ in the case of undirected approaches. The value $\alpha = 0.5$ is the default value adopted in experimental results [12], which is more well balanced configuration. For low values ($\alpha \approx 0.0$), the oriented methods (e.g., *ORFC*) degenerate into their counterpart undirected approaches (e.g., *RFC*), and for high values, the oriented methods may become more sensitive to noise. Nevertheless, the hybrid approach *ORFC+GC* showed the overall best results, demonstrating the importance of hybrid methods, and making clear that, even in these cases, *ORFC* can help to improve the graph cut delineation, and to reduce its running time.

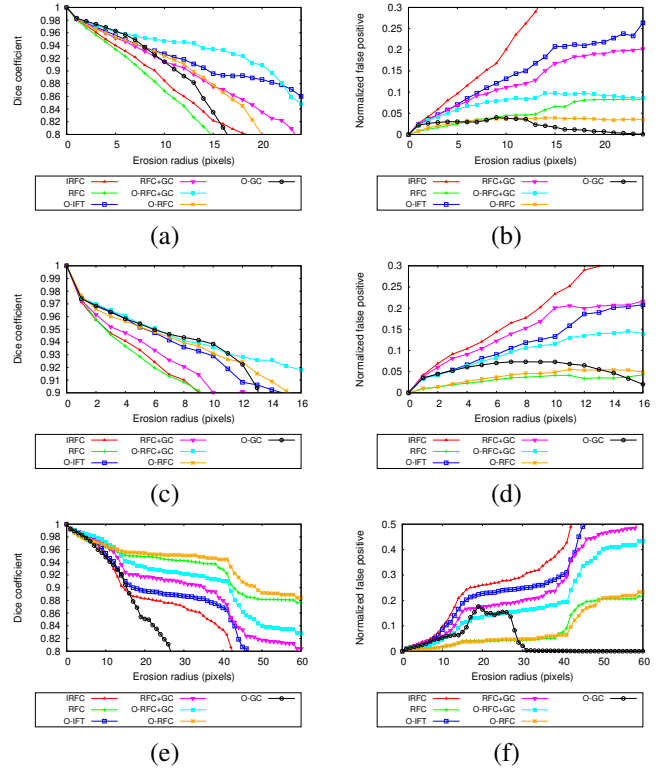


Figure 6. The experimental curves for the 2D datasets. The mean accuracy curves (Dice coefficient of similarity) and the normalized false positive curves, using non-equally eroded-dilated seeds, for segmenting: (a,b) calcaneus, (c,d) talus, and (e,f) liver.

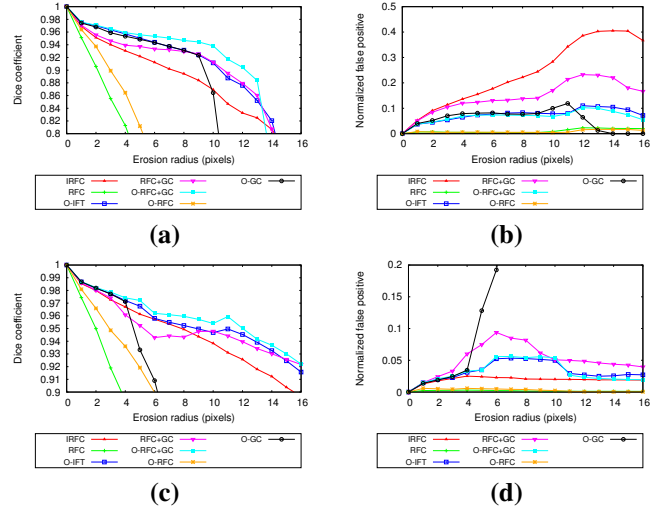


Figure 7. The experimental curves for the 3D datasets. The mean accuracy (Dice coefficient) and normalized false positive curves, using non-equally eroded-dilated seeds, for segmenting: (a,b) cerebellum dataset, and (c,d) skull stripping dataset.

VI. CONCLUSIONS

We introduced the *ORFC* technique and showed that it can effectively exploit the boundary polarity improving the results in relation to its predecessor *RFC*. We also presented

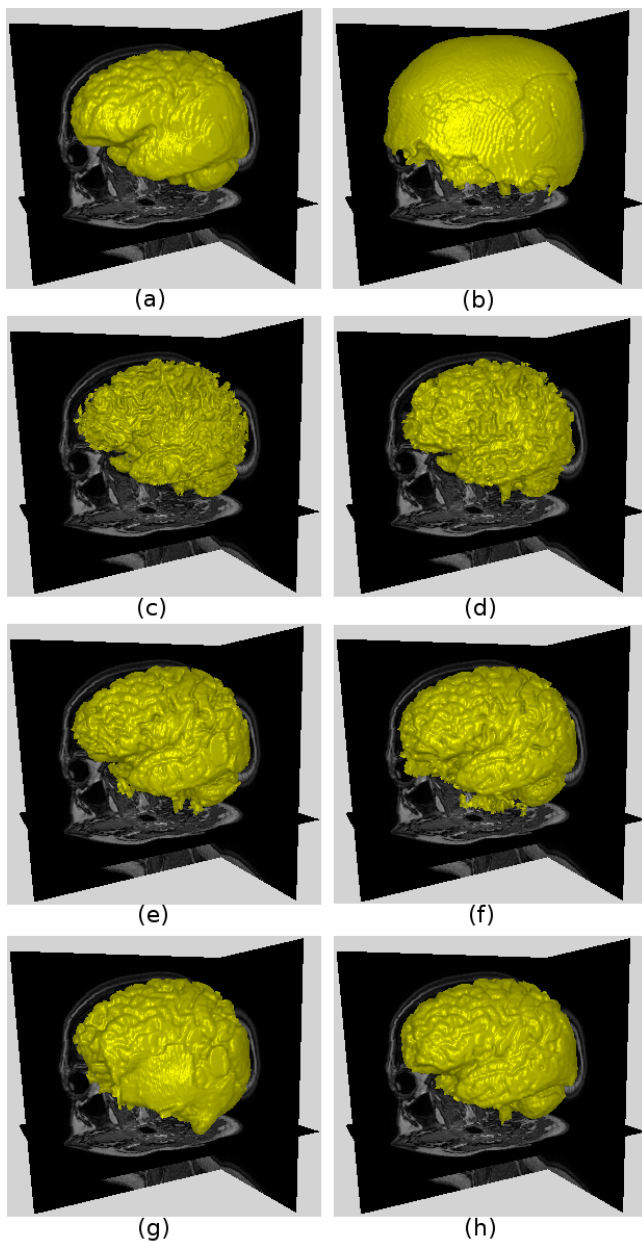


Figure 8. Example of skull stripping. (a) The ground truth. The segmentation results for: (b) OGC, (c) RFC, (d) ORFC, (e) IRFC, (f) OIFT, (g) RFC+GC, and (h) ORFC+GC.

a powerful hybrid approach, which outperforms the previous works [3], [17]. A conference paper was published in SIBGRAPI [18], and one journal paper was published in the EURASIP Journal on Image and Video Processing [19]. As future work, we intend to test the usage of shape constraints in the *ORFC* (similar to what was done in [14]), and to combine the proposed methods with *Fuzzy Object Models* [20], in order to get a fully automatic segmentation result.

ACKNOWLEDGMENT

The author thanks CNPq (305381/2012-1, 486083/2013-6, FINEP 1266/13), FAPESP grant # 2011/50761-2, CAPES, and

Dr. J. K. Udupa (MIPG-UPENN) for the images.

REFERENCES

- [1] K. Ciesielski, J. Udupa, P. Saha, and Y. Zhuge, "Iterative relative fuzzy connectedness for multiple objects with multiple seeds," *Computer Vision and Image Understanding*, vol. 107, no. 3, pp. 160–182, 2007.
- [2] P. Miranda and L. Mansilla, "Oriented image foresting transform segmentation by seed competition," *IEEE Transactions on Image Processing*, vol. 23, no. 1, pp. 389–398, Jan 2014.
- [3] K. C. Ciesielski, P. Miranda, A. Falcão, and J. K. Udupa, "Joint graph cut and relative fuzzy connectedness image segmentation algorithm," *Medical Image Analysis (MEDIA)*, vol. 17, no. 8, pp. 1046–1057, 2013.
- [4] Y. Boykov and G. Funka-Lea, "Graph cuts and efficient N-D image segmentation," *Intl. Jnl. of Comp. Vision*, vol. 70, no. 2, pp. 109–131, 2006.
- [5] A. Falcão, J. Stolfi, and R. Lotufo, "The image foresting transform: Theory, algorithms, and applications," *IEEE Transactions on Pattern Analysis and Machine Intelligence*, vol. 26, no. 1, pp. 19–29, 2004.
- [6] P. Miranda and A. Falcão, "Elucidating the relations among seeded image segmentation methods and their possible extensions," in *XXIV Conference on Graphics, Patterns and Images*, Maceió, AL, Aug 2011, pp. 289–296.
- [7] K. Ciesielski, J. Udupa, A. Falcão, and P. Miranda, "Fuzzy connectedness image segmentation in graph cut formulation: A linear-time algorithm and a comparative analysis," *Journal of Mathematical Imaging and Vision*, vol. 44, no. 3, pp. 375–398, Nov 2012.
- [8] C. Couprie, L. Grady, L. Najman, and H. Talbot, "Power watersheds: A unifying graph-based optimization framework," *IEEE Transactions on Pattern Analysis and Machine Intelligence*, vol. 99, 2010.
- [9] P. Miranda and A. Falcão, "Links between image segmentation based on optimum-path forest and minimum cut in graph," *Journal of Mathematical Imaging and Vision*, vol. 35, no. 2, pp. 128–142, 2009.
- [10] K. Ciesielski, J. Udupa, A. Falcão, and P. Miranda, "A unifying graph-cut image segmentation framework: algorithms it encompasses and equivalences among them," in *Proc. of SPIE on Medical Imaging: Image Processing*, vol. 8314, 2012.
- [11] Y. Boykov and V. Kolmogorov, "An experimental comparison of min-cut/max-flow algorithms for energy minimization in vision segmentation with connectivity priors," in *IEEE Transactions on Pattern Analysis and Machine Intelligence*. IEEE, Set 2004, pp. 1124–1137.
- [12] L. Mansilla and P. Miranda, "Image segmentation by oriented image foresting transform: Handling ties and colored images," in *18th Intl. Conf. on Digital Signal Processing*, Greece, Jul 2013, pp. 1–6.
- [13] D. Singaraju, L. Grady, and R. Vidal, "Interactive image segmentation via minimization of quadratic energies on directed graphs," in *Intl. Conf. on Computer Vision and Pattern Recognition*, Jun 2008, pp. 1–8.
- [14] L. Mansilla and P. Miranda, "Image segmentation by oriented image foresting transform with geodesic star convexity," in *15th International Conference on Computer Analysis of Images and Patterns (CAIP)*, vol. 8047, York, UK, Aug 2013, pp. 572–579.
- [15] P. Saha and J. Udupa, "Relative fuzzy connectedness among multiple objects: Theory, algorithms, and applications in image segmentation," *Comp. Vision and Image Understanding*, vol. 82, no. 1, pp. 42–56, 2001.
- [16] J. Udupa, P. Saha, and R. Lotufo, "Relative fuzzy connectedness and object definition: Theory, algorithms, and applications in image segmentation," *IEEE Transactions on Pattern Analysis and Machine Intelligence*, vol. 24, pp. 1485–1500, 2002.
- [17] K. Ciesielski, P. Miranda, J. Udupa, and A. Falcão, "Image segmentation by combining the strengths of relative fuzzy connectedness and graph cut," in *Proc. of the International Conference on Image Processing*. Orlando, Florida, USA: IEEE, Oct 2012, pp. 2005–2008.
- [18] H. H. C. Bejar and P. A. Miranda, "Oriented relative fuzzy connectedness: Theory, algorithms, and applications in image segmentation," in *27th SIBGRAPI Conference on Graphics, Patterns and Images*, 2014, pp. 304–311.
- [19] H. H. Ccacyahuilca Bejar and P. A. V. Miranda, "Oriented relative fuzzy connectedness: theory, algorithms, and its applications in hybrid image segmentation methods," *EURASIP Journal on Image and Video Processing*, vol. 2015, no. 1, 2015. [Online]. Available: <http://dx.doi.org/10.1186/s13640-015-0067-4>
- [20] J. K. Udupa, K. C. Ciesielski, and A. X. Falcão, "Body wide hierarchical fuzzy modeling, recognition, and delineation of anatomy in medical images," vol. 18. Elsevier Science Inc., Jul 2014, pp. 752–771.